International Journal of Electrical and Computer Engineering (IJECE)
Vol. 7, No. 5, October 2017, pp. 2661~2673
ISSN: 2088-8708, DOI: 10.11591/ijece.v7i5.pp2661-2673

Bit-error-rate Optimization for CDMA Ultra-wideband System Using Generalized Gaussian Approach

Chung Gwo Chin[1], Mohamad Yusoff Alias[2], Tiang Jun Jiat[3]
Faculty of Engineering, Multimedia University, Malaysia

Article Info

Article history:

Received Feb 20, 2017
Revised May 18, 2017
Accepted Jun 11, 2017

Keywords:

Bit-error-rate
Multipath propagation
Statistical distribution
Ultra-wideband

ABSTRACT

Ultra-wideband is a wireless technology arisen for future high speed multimedia applications. It can provide data rate in excess of Gigabits per second by transmitting impulse signal through the free space. However, the ultra-wideband indoor channel models proposed by the IEEE P802.15.3a suffer long multipath propagation. Due to this multipath effect, several studies have been done to improve the bit-error-rate performance of the ultra-wideband system in the existence of severe interference. Yet, most of the proposed algorithms were formulated based on the Gaussian distribution, which is not true in ultra-wideband. In this paper, we first analyze the statistical behavior of the CDMA-UWB signal by applying the Kullback-Leibler divergence index. Based on the analysis, a non-Gaussian equalizer is developed by deriving an enhanced bit-error-rate optimization algorithm using the Generalized Gaussian approach. The proposed equalizer has been shown to achieve a performance gain of at least 1.5dB to 2dB over the other equalizers simulated under IEEE P802.15.3a channel models.

Corresponding Author:

Chung Gwo Chin,
Faculty of Engineering,
Multimedia University,
Persiaran Multimedia, Cyberjaya, 63100 Selangor, Malaysia.
Email: gcchung@mmu.edu.my

1. INTRODUCTION

Ultra-wideband (UWB) is a future potential wireless technology that transmits extremely short duration pulses typically in the range of few nanoseconds or picoseconds [1]. In fact, it can support data rate more than 1 Gigabits per second (Gbps) [2], which is suitable for high speed multimedia applications such as video conferencing, and radar detection [3]. However, the standard UWB indoor channel implemented by IEEE P802.15.3a Wireless Personal Area Networks (WPAN) up to now; still contains a response of 60-200 multipaths [4], which can cause severe inter-symbol interference (ISI) and multi-user access interference (MAI). In order to overcome the multipath effect, Rake collectors have been presented to be effectively resolving the multipath components in UWB channel as well as maximizing the signal-to-noise ratio [5]. Besides that, conventional equalizer such as minimum mean square error (MMSE) equalizer can be used to combine with the Rake collectors for channel estimation as well as interference mitigation as reported in [6].

On the other hand, several studies have shown that the minimum bit error rate (MBER) equalizer is capable to achieve a significant performance gain [7]-[8] against the MMSE equalizer simulated under long multipath channel. In fact, the BER is actually the true performance indicator, not the mean square error (MSE). In [9], an adaptive MBER decision feedback equalizer (DFE) has been implemented to improve the bit-error-rate (BER) performance of a single-user UWB system. The result has been further extended to the recursive MBER DFE as reported in [10]. However, MBER detection algorithm [11]-[12] is formulated based on the statistical behavior of a narrowband channel governed by the central limit theorem, which is a Gaussian distribution. This is not applicable to wideband channel, especially UWB as reported in [13]-[16].

In some of the above studies, Middleton Class-A (MCA) distribution model is found to be a better approach to the statistical distribution of UWB received signal since the UWB system transmits extremely short duration pulses or impulses through the free space channel. MCA is an impulsive noise model formed widely due to intelligent noises that contains non-Gaussian impulsive components [17]. However, other studies also show that the mixture of Gaussian can be used to model the UWB channel in some circumstances. Hence, there is no specific model has been proposed that can be dedicatedly used to represent the statistical behavior of the UWB received signal under different channel conditions. Such distinctive behavior has been demonstrated in IEEE P802.15.3a as channel model 1 (CM1), CM2, CM3 and CM4 [18]. CM1 is the only channel model, which has a clear Line-Of-Sight (LOS) path. On the other hand, CM2, CM3 and CM4 have larger root mean square (RMS) delays due to the absence of LOS paths.

Therefore, the performance of the conventional MBER equalizer will not be optimized [9] in UWB system that exhibits non-Gaussian statistical behavior. In this paper, we propose Generalized Gaussian (GG) distribution [19] to model the statistical behavior of the code division multiple access (CDMA)-UWB signed decision variable (SDV) since the GG model can be used to approximate all different types of distribution models. Statistical comparisons have been done among the Gaussian, MCA and the proposed GG models by using Kullback-Leibler (KL) divergence index [20]. Based on the analysis, we then derive an enhanced BER optimization algorithm based on MBER criterion using both MCA and GG approach. Hence, a non-Gaussian equalizer has been developed to optimize the BER performance under severe MAI interference. Finally, we perform the BER performance comparisons for MMSE, MBER, MCA-MBER and the proposed Generalized (G)-MBER equalizers simulated under the standard channel models of IEEE P802.15.3a [18].

2. SYSTEM MODEL

The system model used in this paper is the CDMA-UWB system, which transmits multi-user UWB signal using the following Equation [1]:

$$s(t) = \sum_{m=1}^{M} g_m(t) d_m(t) \tag{1}$$

where M is the total number of users, $d_m(t)$ is the mth user's UWB signal modulated by binary phase shift keying (BPSK) bit streams, $\{\mathbf{b}_m\} \epsilon \{-1,1\}$ and $g_m(t)$ is the Gold code spreading sequence [21].

The UWB transmitted signal is propagated through the multipath channel model of IEEE P802.15.3a WPAN [18]. At the receiver end, the UWB received signal is given as,

$$r(t) = s(t) * h(t) + n(t) \tag{2}$$

where $h(t)$ is the multipath components, and $n(t)$ is the additive white Gaussian noise (AWGN).

The received signal is then processed by an equalizer [21] and the equalized output is equal to:

$$\mathbf{y} = \mathbf{w}\mathbf{R}^{\mathrm{T}} \tag{3}$$

where $\mathbf{w} = [w_0, w_1, \ldots, w_{L-1}]$ is the equalizer's coefficients with L tap length, and $\mathbf{R}^{\mathrm{T}}$ is the matrix transpose of the sampling output of the received signal, $r(t)$.

Finally, the UWB SDV of the mth desired user can be defined as [9]:

$$y_s = \mathrm{sgn}(\mathbf{b}_m[\mathrm{k}])\mathbf{y}_m[\mathrm{k}] \tag{4}$$

where $\mathbf{y}_m[\mathrm{k}]$ is kth sampled of mth user's equalized signal and $\mathbf{b}_m[\mathrm{k}]$ is the transmitted kth information bit.

3. PROPOSED ALGORITHM

Our proposed optimization algorithm is illustrated in Figure 1. Firstly, we have to choose the most suitable model to model the distribution of the UWB SDV. Based on the previous studies, there are two models have been selected for comparison: GG, and MCA models. MCA model is said to be a better approach in [13]-[15]. However, we will show later that GG is a better approach than MCA model in multi-user UWB environment by analyzing the statistical behavior of the UWB SDV in Section 4. After estimating the unknown parameters of the chosen models, the BER optimized equation can be derived as shown in the

next section. Finally, the optimized equation is used to adapt the equalizer's coefficient for BER optimization of the CDMA-UWB system.

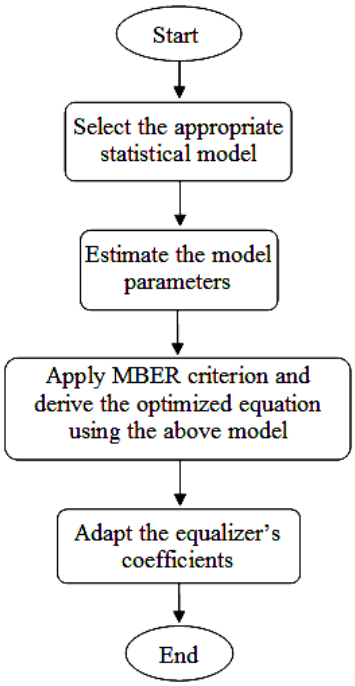

Figure 1. Proposed optimization algorithm flow chart.

3.1. Generalized Gaussian Approach

Based on the assumption that the SDV has an equi-probable probability density function (pdf) [14], which has been verified in the simulated result shown in Section 4, the distribution of a GG model can be written as [19],

$$f_{GG}(y_s;\mathbf{w}) = \frac{A(\beta)}{2S(\sigma_{GG},\beta)\sqrt{\mathbf{w}^{\mathrm{T}}\mathbf{w}}} \cdot e^{-\left(\frac{|y_s - z|}{S(\sigma_{GG},\beta)\sqrt{\mathbf{w}^{\mathrm{T}}\mathbf{w}}}\right)^{\beta}} \tag{5}$$

where σ_{GG} is the variance, β is the shape factor, and the others are defined as following [19]:

$$S(\sigma_{GG},\beta) = \sigma_{GG} \cdot \sqrt{\frac{\Gamma\left(1/\beta\right)}{\Gamma\left(3/\beta\right)}} \tag{6}$$

$$A(\beta) = \frac{\beta}{\Gamma\left(1/\beta\right)} \tag{7}$$

$$z = \mathrm{sgn}(\mathbf{b}_m[\mathrm{k}])\mathbf{y}'_m[\mathrm{k}] \tag{8}$$

where $\mathbf{y}'_m[\mathrm{k}]$ is the k^{th} sampled of noise free equalizer output [9], and $\Gamma(\bullet)$ is the Gamma function.

In order to minimize the BER based on MBER criterion [12], we start to derive our optimization algorithm by first calculating the probability of error, $P_E(\mathbf{w})$ [19] using the GG model stated in Equation (5):

$$P_E(\mathbf{w}) = \int_{-\infty}^{0} f_{GG}(y_s;\mathbf{w})dy_s \cdot \tag{9}$$

Referring to Appendix I, $P_E(\mathbf{w})$ can be simplified to,

$$P_E(\mathbf{w}) = -\frac{A(\beta)}{2}\int_{\infty}^{C(\mathbf{w})} e^{-|x|^{\beta}}dx \cdot \tag{10}$$

The gradient of $P_E(\mathbf{w})$ is then formulated as,

$$\frac{\partial P_E(\mathbf{w})}{\partial \mathbf{w}} = -\frac{A(\beta)}{2}\frac{\partial}{\partial \mathbf{w}}\int_{\infty}^{C(\mathbf{w})} e^{-|x|^{\beta}}dx \cdot \tag{11}$$

Upon solving the integral term as shown in Appendix I, the gradient of $P_E(\mathbf{w})$ can be written in the form of,

$$\Delta P_E(\mathbf{w}) = -\frac{A(\beta)}{2S(\sigma_{GG},\beta)} e^{-\left(\frac{|z|}{S(\sigma_{GG},\beta)\sqrt{\mathbf{w}^{\mathrm{T}}\mathbf{w}}}\right)^{\beta}} \times \left[\frac{\mathbf{w}^{\mathrm{T}}\mathbf{w}\mathbf{I} - \mathbf{w}\mathbf{w}^{\mathrm{T}}}{(\mathbf{w}^{\mathrm{T}}\mathbf{w})^{3/2}}\right] \mathrm{sgn}(\mathbf{b}_m[\mathrm{k}])\mathbf{R}_m^{'\,\mathrm{T}} \cdot \tag{12}$$

To obtain a unique solution, we can let $\mathbf{w} = \frac{\mathbf{w}}{\sqrt{\mathbf{w}^T\mathbf{w}}}$ [11], so that it is restricted to a length of unity magnitude.

$$\Delta P_E(\mathbf{w}) = \frac{A(\beta)}{2S(\sigma_{GG},\beta)} e^{-\left(\frac{|z|}{S(\sigma_{GG},\beta)}\right)^{\beta}} \times \mathrm{sgn}(\mathbf{b}_m[\mathrm{k}])\left[\mathbf{w}\mathbf{w}^{\mathrm{T}} - \mathbf{I}\right]\mathbf{R}_m^{'\,\mathrm{T}} \cdot \tag{13}$$

By replacing the variance with radius factor [7], $\rho_{GG} = K\sigma_{GG}$, we can obtain the final BER optimized equation in the form of,

$$\Delta P_E(\mathbf{w}) = \frac{A(\beta)}{2S(\rho_{GG},\beta)} e^{-\left(\frac{|z|}{S(\rho_{GG},\beta)}\right)^{\beta}} \times \mathrm{sgn}(\mathbf{b}_m[\mathrm{k}])[\mathbf{w}^{\mathrm{T}}\mathbf{y}_m^{'}[\mathrm{k}] - \mathbf{R}_m^{'\,\mathrm{T}}] \tag{14}$$

where K is the radius factor introduced for experimental purpose as shown in Section 4.

3.2. Middleton Class-A Approach

For the second approach, we can derive the BER optimization using the same method. The pdf of the simplified MCA distribution is given as [17],

$$f_{MCA}(y_s;\mathbf{w}) = \frac{Ae^{-A}}{\sqrt{4\pi\sigma_{MCA}^2\mathbf{w}^{\mathrm{T}}\mathbf{w}}} \cdot e^{-\left(\frac{(y_s - z)^2}{4\sigma_{MCA}^2\mathbf{w}^{\mathrm{T}}\mathbf{w}}\right)} \tag{15}$$

where $2\sigma_{MCA}^2 = \frac{1/A + \zeta}{1+\zeta}$, A is the overlap index in the range of $10^{-4} \le A \le 1$, and

$$\zeta = \frac{\Omega_A}{\Omega_G} \tag{16}$$

is the Gaussian factor in the range of $10^{-6} \le \zeta \le 1$ with non-Gaussian intensity, Ω_A, and Gaussian intensity, Ω_G.

We again derive our optimization algorithm by first calculating the probability of error, $P_E(\mathbf{w})$ using the MCA model stated in Equation (15):

$$P_E(\mathbf{w}) = \int_{-\infty}^{0} f_{MCA}(y_s;\mathbf{w})dy_s . \tag{17}$$

Referring to Appendix II, $P_E(\mathbf{w})$ can be simplified to,

$$P_E(\mathbf{w}) = -\frac{Ae^{-A}}{\sqrt{4\pi}} \int_{\infty}^{D(\mathbf{w})} e^{-\frac{x^2}{4}} dx . \tag{18}$$

The gradient of $P_E(\mathbf{w})$ is then formulated as,

$$\frac{\partial P_E(\mathbf{w})}{\partial \mathbf{w}} = -\frac{Ae^{-A}}{\sqrt{4\pi}} \frac{\partial}{\partial \mathbf{w}} \int_{\infty}^{D(\mathbf{w})} e^{-\frac{x^2}{4}} dx . \tag{19}$$

Upon solving the integral term as shown in Appendix II, $\Delta P_E(\mathbf{w})$ can be written in the form of,

$$\Delta P_E(\mathbf{w}) = -\frac{Ae^{-A}}{\sqrt{4\pi\sigma_{MCA}^2}} e^{-\left(\frac{\mathbf{y}_m'[k]^2}{4\sigma_{MCA}^2\mathbf{w}^T\mathbf{w}}\right)} \times \left[\frac{\mathbf{w}^T\mathbf{w}\mathbf{I} - \mathbf{w}\mathbf{w}^T}{(\mathbf{w}^T\mathbf{w})^{3/2}}\right] \mathrm{sgn}(\mathbf{b}_m[k])\mathbf{R}_m'^T . \tag{20}$$

To obtain a unique solution, we can again constraint the equalizer's coefficient matrix, **w** to have a unity length [11]. The final BER optimized equation is then derived as:

$$\Delta P_E(\mathbf{w}) = \frac{Ae^{-A}}{\sqrt{4\pi\sigma_{MCA}^2}} e^{-\frac{\mathbf{y}_m'[k]^2}{4\sigma_{MCA}^2}} \times \mathrm{sgn}(\mathbf{b}_m[k])[\mathbf{w}^T\mathbf{y}_m'[k] - \mathbf{R}_m'^T] . \tag{21}$$

Finally, the coefficients of the equalizer in Equation (14) and Equation (21) can be easily adapted by an adaptive algorithm [21]. Since both GG and MCA approaches have linear equations, which require only single iteration in each adaptation; the computational complexity should not differ much from the conventional MMSE. However, the shape factor, β of GG model and the overlap index, A of MCA model have to be estimated as illustrated in the next section.

4. RESULT AND DISCUSSION

We present results simulated under IEEE P802.15.3a WPAN channel models including CM1, CM2, and CM4 [18]. Simulations are performed over N_c = 100 channel realizations in the existence of AWGN noise using MATLAB v2010 software. The Gold code used for the CDMA-UWB system has a sequence length of 31 in order to have a better cross correlation property [21]. For fair comparison, all of the simulated equalizers uses steepest decent adaptive algorithm [21] to adapt its own coefficients.

4.1. Parameter Estimation

Since GG and MCA models have been chosen in our optimization algorithm for comparison, we have to estimate the shape factor, β of GG model and the overlap index, A of MCA model. Figure 2(a) shows the shape factor estimation of GG model under CM1 using maximum likelihood estimation (MLE) [22]. According to the gradient of shape factor, we can obtain the maximum likelihood at $\beta \approx 1.85$ when the magnitude of gradient approaches zero. The same method has been applied to CM2 and CM4, and the estimated shape factors are shown in Table 1. Notice that all UWB channels except CM2, exhibits non-Gaussian behaviors because the estimated shape factors are around 1.85 to 1.86. On the other hand, CM2 has an estimated $\beta \approx 1.98$, which is close to the shape factor of Gaussian distribution (β = 2). Since the estimated shape factors under CM1 and CM4 are almost the same, we have chosen β = 1.85 as our parameter under these two channels for simplicity throughout the simulation.

Figure 2(b) shows the overlap index estimation of MCA model under CM1 using Kullback-Leibler (KL) divergence index [20], which is equal to:

$$KL = \sum_{i=-\infty}^{\infty} P_i \log \frac{P_i}{Q_i} \text{ [dB]} \quad (22)$$

where P_i is the statistical probability of CDMA-UWB SDV, Q_i is the statistical probability of the tested model, which is the MCA model in this case. KL divergence index is used to measure the difference between two statistical models; in which lower index indicates higher similarity between these two tested probability models. It can be observed that the performance of the KL divergence index reduces drastically by decreasing the overlap index, A. Eventually, it is found that there is not much performance improvement when $A < 0.01$. Similar results have been obtained for the KL divergence index simulated under CM2 and CM4. Hence, we have chosen $A = 0.001$ as our parameter under all channels throughout the simulation.

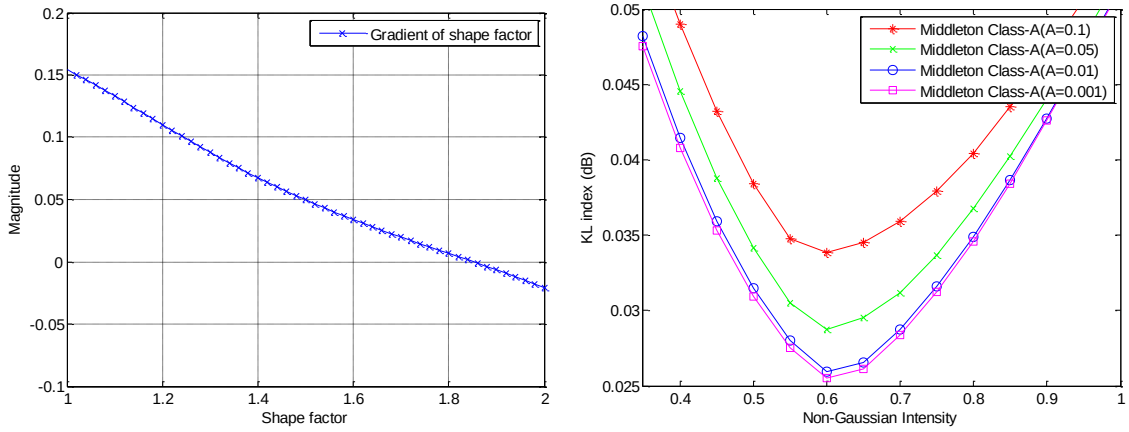

(a) (b)

Figure 2. (a) Shape factor estimation of GG, and (b) overlap index estimation of MCA models under CM1.

Table 1. Estimated shape factor of GG model under CM1, CM2, and CM4.

Estimated Parameter	CM1	CM2	CM4
Shape factor	1.8516	1.9766	1.8619

4.2. Statistical Analysis

In order to show that the proposed GG model is a better approach than the MCA model for CDMA-UWB system, we perform the statistical analysis on the UWB SDV and compare it to the Gaussian, GG and MCA models. Figure 3 shows the statistical distribution of CDMA-UWB SDV, Gaussian, MCA and GG models in the existence of MAI under CM1 at E_b/N_o = 15 dB. Since CM1 has the most significant components at the first few channel multipaths [18], the distribution of UWB SDV exhibits slightly "impulse" behavior. Hence, the GG model ($\beta = 1.85$), which has a slightly "impulse" distribution is found to be a better fit to the distribution of UWB SDV as compared to the Gaussian ($\beta = 2$) and MCA ($\Omega_A = 0.6$).

Furthermore, this result has been further verified using the KL divergence index by varying the non-Gaussian factor, Ω_A and the radius factor, K accordingly. Figure 4 shows the KL divergence index comparisons of CDMA-UWB SDV, MCA and GG models in the existence of MAI under CM1, CM2, and CM4 at E_b/N_o = 15 dB. In Figure 4(a), GG has attained the lowest KL index (0.0243 dB) among all the results at $K = 1.25$; where else the Gaussian has the same performance (0.0255 dB) as the MCA. The KL divergence index of MCA has been offset horizontally for better comparisons. So, the actual lowest KL index of MCA occurs at $\Omega_A = 0.6$. The same verification method has been applied to CM2 and CM4 as illustrated in Figure 4(b), and 4(c), and the lowest KL divergence index performance has been summarized in Table 2. It is shown that the GG has remained the lowest KL index performance (0.0248 dB) under CM4 at $K = 1.35$ as compared to the Gaussian and MCA since CM4 exhibits slightly "impulse" behavior such as reported under CM1.

However, all models achieve the same KL index performance (0.023 dB) under CM2 because it has a nearly Gaussian statistical behavior as stated in previous section.

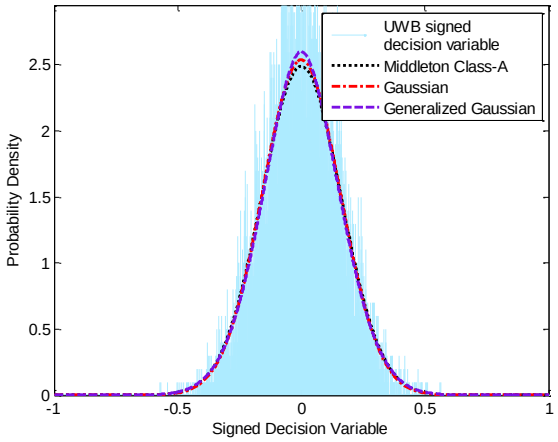

Figure 3. Statistical distribution of UWB SDV, MCA, Gaussian, and GG models under CM1.

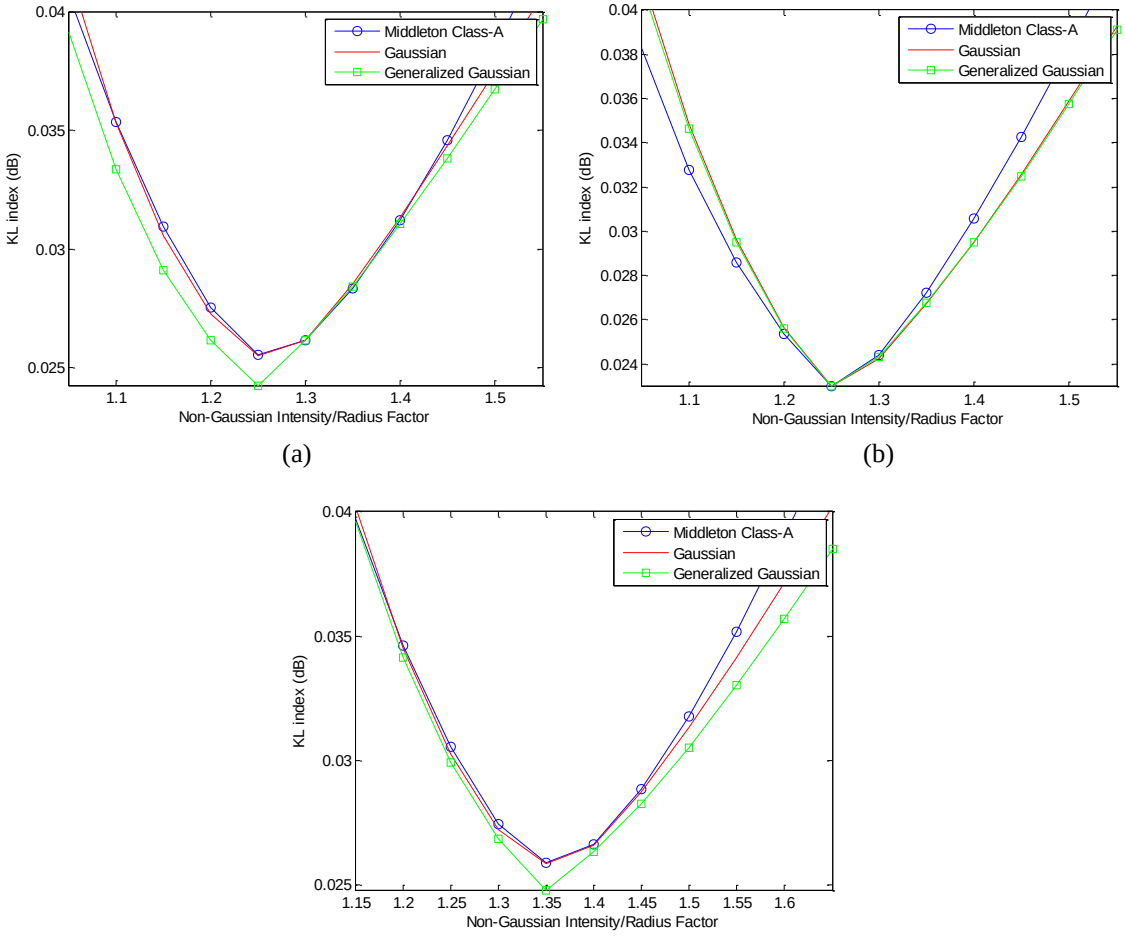

Figure 4. KL divergence index comparisons of UWB SDV, MCA, Gaussian, and GG models under (a) CM1, (b) CM2, and (c) CM4.

Table 2. KL index performance (lowest) of Gaussian, MCA and GG models under CM1, CM2, and CM4.

Distribution Models	CM1	CM2	CM4
Gaussian	0.0255dB (K = 1.25)	0.023dB (K = 1.25)	0.0259dB (K = 1.35)
MCA	0.0255dB (Ω_A = 0.6)	0.023dB (Ω_A = 0.6)	0.0255dB (Ω_A = 0.55)
GG	0.0243dB (K = 1.25)	0.023dB (K = 1.25)	0.0248dB (K = 1.35)

4.3. Performance Comparisons

Last but not least, we conduct the performance comparisons among the MMSE, MBER, MCA-MBER and our proposed G-MBER equalizers. Table 3 shows the average computational time per iteration of each algorithm used by the equalizers mentioned above. The result is simulated using 2.16GHz Intel(R) Celeron(R) Processor with 2GB memory and is averaged over 100,000 of iterations. It is shown that the MMSE has the fastest computation time; where else the MCA-MBER has the slowest time. However, both the MBER and our proposed G-MBER require almost the same computational time. Although the G-MBER needs around 30 percentages more computational time than the MMSE, it can achieve significant BER performance improvement over the MMSE as show in the next results.

Table 3. Average computational time of MMSE, MBER, MCA-MBER and G-MBER equalizers.

Average Computational Time	MMSE	MBER	MCA-MBER	G-MBER
1 iteration	1.9703×10^{-5}s	2.5792×10^{-5}s	1.0004×10^{-4}s	2.6318×10^{-5}s

Hence, we further simulate and compare the BER performances of the MMSE, MBER, MCA-MBER, and proposed G-MBER equalizers as shown in Figure 5. The result is simulated at a data rate of 1800 Mbps, 100 Mbps, and 65 Mbps respectively under CM1, CM2 and CM4 for CDMA-UWB system. The radius factor and non-Gaussian intensity are set accordingly as shown in Table 2. The equalizer's tap length is set to a minimum of 7 in order to capture all significant components in the UWB channel multipath. The step size used for the adaptation process is chosen as small as 0.005 to minimize the propagation error. The number of multiple users simulated is restricted to 8 only for CM1; and 4 only for CM2, and CM4 since these are the maximum number of users can be supported by CDMA-UWB system without channel coding [21].

In Figure 5 (a), notice that the proposed G-MBER outperforms the BER performance of the MMSE, MBER, and MCA-MBER under CM1. At a BER of 10^{-7}, G-MBER achieves a performance gain of about 2 dB compared to the MBER and MCA-MBER. However, the MMSE does not achieve BER of 10^{-7} at $E_b/N_o <$ 25 dB. It is interesting to see that the MBER and MCA-MBER have almost the same BER performance since both equalizers utilize the Gaussian and MCA distribution in their optimization algorithms, which show an approximate KL divergence index performance as presented in Figure 4 (a). Similar result has been obtained for CM4 as shown in Figure 5 (c) since it has a channel behavior almost same as CM1 as presented in Table 1. It can be observed that the G-MBER achieve a performance gain of approximately 1.5 dB as compared to the MBER and MCA-MBER at a BER of 10^{-7}. However, this performance improvement cannot be attained under CM2 as shown in Figure 5 (b). At a BER of 10^{-7}, the G-MBER, MBER, and MCA-MBER obtain the same performance gain of about 1 dB as compared to the MMSE. This result has been expected since CM2 is a UWB channel model that exhibits nearly Gaussian distribution behavior as illustrated in Figure 4 (b).

Finally, we can say that the BER performance of the UWB system is affected by the statistical model that used to derive the optimized equation for the equalizer. Since CDMA-UWB system exhibits non-Gaussian behavior in CM1, and CM4, but not in CM2, the proposed G-MBER equalizer is more preferable to be used to optimize the BER performance of the UWB system simulated under different channel conditions.

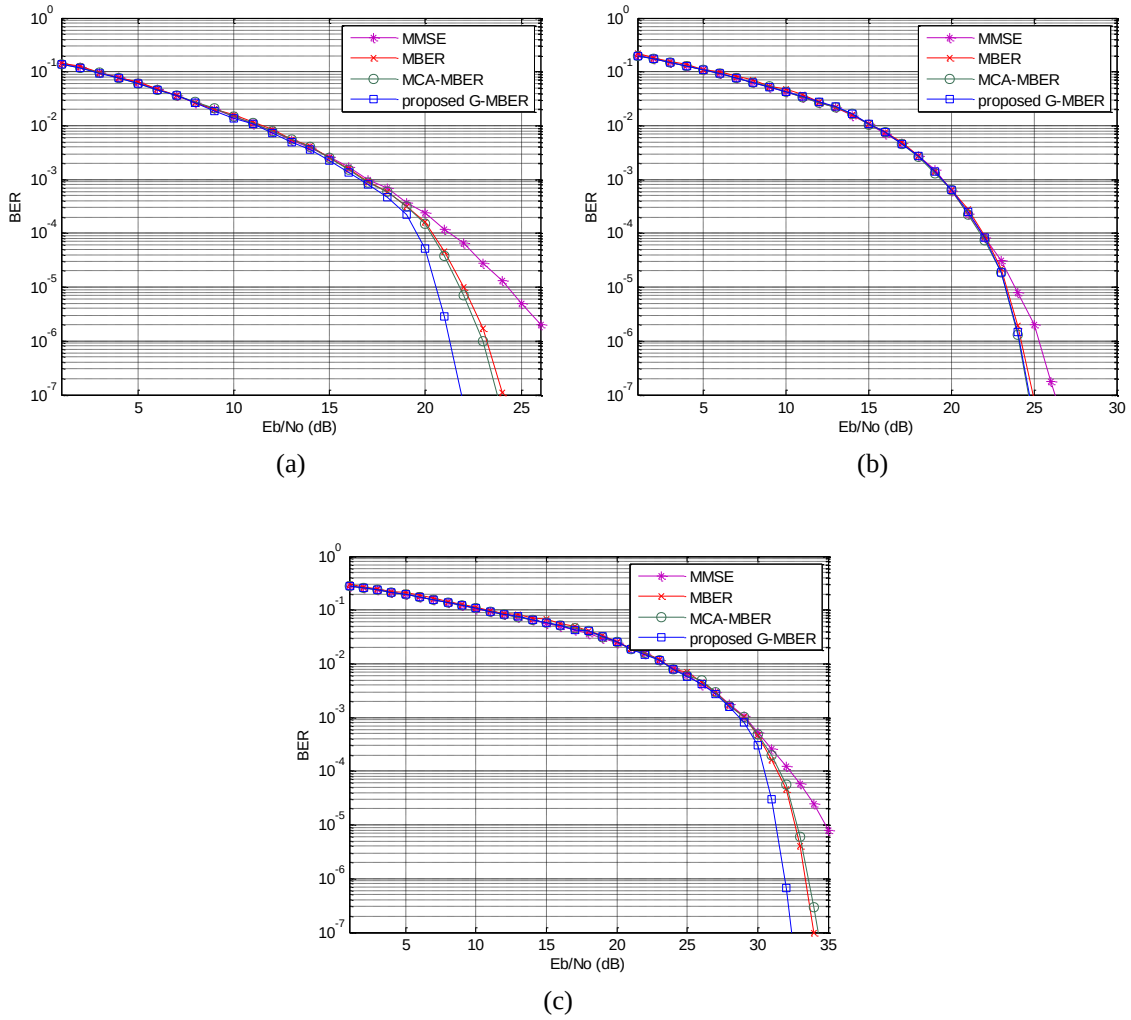

Figure 5. BER performance comparisons of MMSE, MBER, MCA-MBER, and G-MBER equalizers under (a) CM1, (b) CM2, and (c) CM4.

5. CONCLUSION

The statistical distribution of CDMA-UWB signed decision variable has been studied in the presence of multi-user access interference. Simulation results show that the Generalized Gaussian is more suitable to model the variation of statistical behavior of the UWB signal in different environment. Based on the analysis, an enhanced bit-error-rate optimization algorithm based on MBER criterion has been derived and hence, a non-Gaussian equalizer has been developed. It has been shown that the proposed equalizer attains a considerable BER performance improvement over the conventional Gaussian and MCA-MBER equalizers simulated under UWB channels that exhibit non-Gaussian behaviors. Further investigation can be done on other types of non-Gaussian system using the proposed equalizer in future.

REFERENCES

[1] Enami S. An UWB Communication Systems: Conventional and 60Hz. 1st ed. Springer, New York. 2013.
[2] Gomes J, Mishra BK. Performance Evaluation of UWB Wireless Link. *International Journal of Information and Network Security*. 2012; 1(3); 188-199.
[3] Darif A, *et al.* IR-UWB: An Ultra Low Power Consumption Wireless Communication Technologie for WSN. *Indonesian Journal of Electrical Engineering*. 2014; 12(8); 5699-5708.
[4] Pascal P, *et al.* Ultra Wide Band Radio Propagation Channel. 1st ed. Wiley, Paris. 2013.
[5] Aimilia PD, *et al.* Increasing The Efficiency of Rake Receivers for Ultra-Wideband Applications. *Wireless Personal Communications*. 2012; 62(3); 715-728.
[6] Zahra A. Design of Pre-Rake DS-UWB Downlink with Pre-equalization. *IEEE Transactions on* Communications. 2012; 60(2); 1-4.

[7] Kovacs L, *et al.* Approximate Minimum Bit Error Rate Equalization for Fading Channels. *EURASIP J. Adv. Signal Process*. 2010; 2010(1); 1-9.
[8] Xufang L, *et al. Minimum-BER Linear Multiuser Detection for DS-CDMA Signals under Impulsive Noise Environments*. 3rd International Conference on Intelligent Control and Information Processing (ICICIP). Dalian, China. 2012; 503-506.
[9] Chung GC, *et al.* An Adaptive Minimum Bit-error-rate Decision Feedback Equalizer for UWB Systems. *IEICE Electronics Express*. 2007; 4(14); 435-441.
[10] Chung GC. Performance of A Recursive MBER Decision Feedback Equalizer in Long Multipath Channel. *IEICE Electronics Express*. 2012; 9(14); 1201-1207.
[11] Chen S. Least Bit Error Rate Adaptive Multi-user Detection. 1st ed. Springer, Southampton. 2013.
[12] Chen S, *et al.* Adaptive Minimum Error-rate Filtering Design: A Review. *IEEE Transactions on Signal Processing*. 2008; 88(7); 1671-1679.
[13] Abed D, Redadaa S. *Statistical Modelling of TR-UWB System under MUI and Impulsive S--S Interference*. International Symposium on Wireless Communication Systems (ISWCS). Paris, France. 2012; 790-794.
[14] Chung GC, *et al. Statistical Distribution of UWB Signals in The Presence of Inter-symbol Interference*. IEEE Conference on Sustainable Utilization and Development in Engineering and Technology (CSUDET). 2013; 60-62.
[15] Bo H, Beaulieu NC. *On Characterizing Multiple Access Interference in TH-UWB Systems with Impulsive Noise Models*. IEEE Radio and Wireless Symposium. Florida, USA. 2008; 879-882.
[16] Tomaso E. A Low-complexity Receiver for Impulse Radio Based upon A Gaussian Mixture Interference Model. *IEEE Transactions on Wireless Communications*. 2008; 7(12); 4967-4876.
[17] Middleton D. Non-Gaussian Statistical Communication Theory. 1st ed. Wiley, New York. 2012.
[18] Foerster JR. IEEE 802.15.SG3a Channel Modeling Subcommittee Report Final. *IEEE 802.15*.SG3a. 2002.
[19] Jean-rene B, *et al.* Mathematical Basis of Statistics. 1st ed. Academic Press, Paris. 2014.
[20] Burnhem KP, Anderson DR. Model Selection and Multi-model Interference. 2nd ed. Springer, New York. 2003.
[21] Gerard B, Maurice C. Digital Signal and Image Processing Using MATLAB. 2nd ed. Wiley, Paris. 2015.
[22] Frederic P, *et al.* Parameter Estimation for Multivariate Generalized Gaussian Distributions. *IEEE Transactions on Signal Processing*. 2013; 61(23); 5960-5971.

BIOGRAPHIES OF AUTHORS

Chung Gwo Chin obtained Bachelor of Electronics Engineering (Hons.) majoring in Telecommunications from Multimedia University, Malaysia in 2005. He then received his MEngSc. from the same university in 2009. He is currently a Lecturer at the Faculty of Engineering, Multimedia University. His research area includes the field of wireless communications especially in UWB, digital signal processing, and interference suppression.

Mohamad Yusoff Alias obtained Bachelor of Science in Engineering (Electrical Engineering) degree from the University of Michigan, Ann Arbor, in May 1998. He then received his Ph.D. degree in December 2004 from the School of ECS, University of Southampton in the United Kingdom. He is currently a Professor at the Faculty of Engineering, Multimedia University in Malaysia. His research interests cover the field of wireless communications especially in OFDM, multiple antenna system, multi-user detection, genetic algorithms in communications, and visible light communication.

Tiang Jun Jiat obtained his first degree in electronics engineering from Multimedia University, Malaysia in 2004. He earned his Master degree from Department of Electrical and Electronics Engineering, University of Science, Malaysia (USM) in 2006. He completed his Ph.D. degree in electrical, electronic& systems engineering at the National University of Malaysia (UKM), Malaysia in 2014. He is currently attached to Faculty of Engineering, Multimedia University, Malaysia as a senior lecturer and researcher. His interests include antenna and propagation, microwave circuits and smart antenna.

APPENDIX I

The probability of error derived using GG model is:

$$P_E(\mathbf{w}) = \int_{-\infty}^{0} \frac{A(\beta)}{2S(\sigma_{GG},\beta)\sqrt{\mathbf{w}^{\mathrm{T}}\mathbf{w}}} e^{-\left(\frac{|y_s - z|}{S(\sigma_{GG},\beta)\sqrt{\mathbf{w}^{\mathrm{T}}\mathbf{w}}}\right)^{\beta}} dy_s . \quad (23)$$

By letting $x = \frac{y_s - z}{S(\sigma_{GG},\beta)\sqrt{\mathbf{w}^{\mathrm{T}}\mathbf{w}}}$,

$$dx = \frac{1}{S(\sigma_{GG},\beta)\sqrt{\mathbf{w}^{\mathrm{T}}\mathbf{w}}} dy_s \quad (24)$$

$$dy_s = S(\sigma_{GG},\beta)\sqrt{\mathbf{w}^{\mathrm{T}}\mathbf{w}}dx. \quad (25)$$

Replacing dy_s into Equation (23) yields,

$$P_E(\mathbf{w}) = \int_{-\infty}^{-C(w)} \frac{A(\beta)S(\sigma_{GG},\beta)\sqrt{\mathbf{w}^{\mathrm{T}}\mathbf{w}}}{2S(\sigma_{GG},\beta)\sqrt{\mathbf{w}^{\mathrm{T}}\mathbf{w}}} \cdot e^{-|x|^{\beta}} dx$$

$$= \frac{A(\beta)}{2} \int_{-\infty}^{-C(\mathbf{w})} e^{-|x|^{\beta}} dx \quad (26)$$

where $C(\mathbf{w}) = \frac{z}{S(\sigma_{GG},\beta)\sqrt{\mathbf{w}^{\mathrm{T}}\mathbf{w}}}$.

Due to equi-probable distribution,

$$P_E(\mathbf{w}) = -\frac{A(\beta)}{2} \int_{\infty}^{C(\mathbf{w})} e^{-|x|^{\beta}} dx \quad (27)$$

The gradient of $P_E(\mathbf{w})$ is then formulated as,

$$\frac{\partial P_E(\mathbf{w})}{\partial \mathbf{w}} = -\frac{A(\beta)}{2} \frac{\partial}{\partial \mathbf{w}} \int_{\infty}^{C(\mathbf{w})} e^{-|x|^{\beta}} dx. \quad (28)$$

Applying the Chain Rule [20], we get:

$$\Delta P_E(\mathbf{w}) = -\frac{A(\beta)}{2} \cdot e^{-|C(\mathbf{w})|^{\beta}} \cdot \frac{\partial}{\partial \mathbf{w}} C(\mathbf{w}) . \quad (29)$$

Upon solving the derivative term,

$$\frac{\partial C(\mathbf{w})}{\partial \mathbf{w}} = \frac{\partial}{\partial w} \frac{\mathrm{sgn}(\mathbf{b}_m[\mathrm{k}])\mathbf{w}\mathbf{R}_m^{'\mathrm{T}}}{S(\sigma_{GG},\beta)\sqrt{\mathbf{w}^{\mathrm{T}}\mathbf{w}}}$$

$$= \frac{\text{sgn}(\mathbf{b}_m[\text{k}])}{S(\sigma_{GG},\beta)} \times \left[\frac{\sqrt{\mathbf{w}^{\text{T}}\mathbf{w}}\frac{\partial}{\partial \mathbf{w}}\mathbf{w}\mathbf{R}_m^{'\,\text{T}} - \mathbf{w}\mathbf{R}_m^{'\,\text{T}}\frac{\partial}{\partial \mathbf{w}}\sqrt{\mathbf{w}^{\text{T}}\mathbf{w}}}{\mathbf{w}^{\text{T}}\mathbf{w}} \right]$$

$$= \frac{\text{sgn}(\mathbf{b}_m[\text{k}])}{S(\sigma_{GG},\beta)} \times \left[\frac{\sqrt{\mathbf{w}^{\text{T}}\mathbf{w}}\mathbf{R}_m^{'\,\text{T}} - \frac{\mathbf{w}\mathbf{R}_m^{'\,\text{T}}}{2\sqrt{\mathbf{w}^{\text{T}}\mathbf{w}}}\frac{\partial}{\partial \mathbf{w}}\mathbf{w}^{\text{T}}\mathbf{w}}{\mathbf{w}^{\text{T}}\mathbf{w}} \right]$$

$$= \frac{\text{sgn}(\mathbf{b}_m[\text{k}])}{S(\sigma_{GG},\beta)} \times \left[\frac{\sqrt{\mathbf{w}^{\text{T}}\mathbf{w}}\mathbf{R}_m^{'\,\text{T}} - \mathbf{w}\mathbf{R}_m^{'\,\text{T}}\frac{\mathbf{w}^{\text{T}}\mathbf{I}}{\sqrt{\mathbf{w}^{\text{T}}\mathbf{w}}}}{\mathbf{w}^{\text{T}}\mathbf{w}} \right]$$

$$= \frac{\text{sgn}(\mathbf{b}_m[\text{k}])}{S(\sigma_{GG},\beta)} \left[\frac{\mathbf{w}^{\text{T}}\mathbf{w}\mathbf{I} - \mathbf{w}\mathbf{w}^{\text{T}}}{(\mathbf{w}^{\text{T}}\mathbf{w})^{3/2}} \right] \cdot \mathbf{R}_m^{'\,\text{T}} \tag{30}$$

where $\mathbf{R}'_m{}^{\text{T}}$ is the matrix transpose of m[th] user's noise free signal. By substituting $\mathbf{C}(\mathbf{w})$ and Equation (30) into Equation (29), we obtain:

$$\Delta P_E(\mathbf{w}) = -\frac{A(\beta)}{2S(\sigma_{GG},\beta)} e^{-\left(\frac{|z|}{S(\sigma_{GG},\beta)\sqrt{\mathbf{w}^{\text{T}}\mathbf{w}}}\right)^{\beta}} \times \left[\frac{\mathbf{w}^{\text{T}}\mathbf{w}\mathbf{I} - \mathbf{w}\mathbf{w}^{\text{T}}}{(\mathbf{w}^{\text{T}}\mathbf{w})^{3/2}} \right] \text{sgn}(\mathbf{b}_m[\text{k}])\mathbf{R}_m^{'\,\text{T}} . \tag{31}$$

APPENDIX II

The probability of error derived using MCA model is:

$$P_E(\mathbf{w}) = \int_{-\infty}^{0} \frac{Ae^{-A}}{\sqrt{4\pi\sigma_{MCA}^2\mathbf{w}^{\text{T}}\mathbf{w}}} \cdot e^{-\left(\frac{(y_s-z)^2}{4\sigma_{MCA}^2\mathbf{w}^{\text{T}}\mathbf{w}}\right)} dy_s . \tag{32}$$

By letting $x = \frac{y_s - z}{\sqrt{\sigma_{MCA}^2\mathbf{w}^{\text{T}}\mathbf{w}}}$,

$$dx = \frac{1}{\sqrt{\sigma_{MCA}^2\mathbf{w}^{\text{T}}\mathbf{w}}} dy_s \tag{33}$$

$$dy_s = \sqrt{\sigma_{MCA}^2\mathbf{w}^{\text{T}}\mathbf{w}}dx . \tag{34}$$

Replacing dy_s into Equation (32) yields,

$$P_E(\mathbf{w}) = \int_{-\infty}^{-D(\mathbf{w})} \frac{Ae^{-A}\sqrt{\sigma_{MCA}^2\mathbf{w}^{\mathrm{T}}\mathbf{w}}}{\sqrt{4\pi\sigma_{MCA}^2\mathbf{w}^{\mathrm{T}}\mathbf{w}}} \cdot e^{-\frac{x^2}{4}} dx$$

$$= \frac{Ae^{-A}}{\sqrt{4\pi}} \int_{-\infty}^{-D(w)} e^{-\frac{x^2}{4}} dx \quad (35)$$

where $D(\mathbf{w}) = \frac{z}{\sigma_{MCA}\sqrt{\mathbf{w}^{\mathrm{T}}\mathbf{w}}}$.

Due to equi-probable distribution,

$$P_E(\mathbf{w}) = -\frac{Ae^{-A}}{\sqrt{4\pi}} \int_{\infty}^{D(\mathbf{w})} e^{-\frac{x^2}{4}} dx. \quad (36)$$

The gradient of $P_E(w)$ is then formulated as,

$$\frac{\partial P_E(\mathbf{w})}{\partial \mathbf{w}} = -\frac{Ae^{-A}}{\sqrt{4\pi}} \frac{\partial}{\partial \mathbf{w}} \int_{\infty}^{D(\mathbf{w})} e^{-\frac{x^2}{4}} dx. \quad (37)$$

Applying the Chain Rule [20], we get:

$$\Delta P_E(\mathbf{w}) = -\frac{Ae^{-A}}{\sqrt{4\pi}} \cdot e^{-\frac{D(\mathbf{w})^2}{4}} \cdot \frac{\partial}{\partial \mathbf{w}} D(\mathbf{w}). \quad (38)$$

Upon solving the derivative term using the same method as in Equation (30),

$$\frac{\partial D(\mathbf{w})}{\partial \mathbf{w}} = \frac{\mathrm{sgn}(\mathbf{b}_m[\mathrm{k}])}{\sigma_{MCA}} \left[\frac{\mathbf{w}^{\mathrm{T}}\mathbf{w}\mathbf{I} - \mathbf{w}\mathbf{w}^{\mathrm{T}}}{(\mathbf{w}^{\mathrm{T}}\mathbf{w})^{3/2}} \right] \cdot \mathbf{R}_m^{'\,\mathrm{T}}. \quad (39)$$

By substituting $D(\mathbf{w})$ and Equation (39) into Equation (38), we obtain:

$$\Delta P_E(\mathbf{w}) = -\frac{Ae^{-A}}{\sqrt{4\pi\sigma_{MCA}^2}} e^{-\left(\frac{\mathbf{y}_m'[\mathrm{k}]^2}{4\sigma_{MCA}^2\mathbf{w}^{\mathrm{T}}\mathbf{w}}\right)} \times \left[\frac{\mathbf{w}^{\mathrm{T}}\mathbf{w}\mathbf{I} - \mathbf{w}\mathbf{w}^{\mathrm{T}}}{(\mathbf{w}^{\mathrm{T}}\mathbf{w})^{3/2}} \right] \mathrm{sgn}(\mathbf{b}_m[\mathrm{k}])\mathbf{R}_m^{'\,\mathrm{T}}. \quad (40)$$